iScience

CellPress
OPEN ACCESS

Article

Mechanically sensitive HSF1 is a key regulator of left-right symmetry breaking in zebrafish embryos

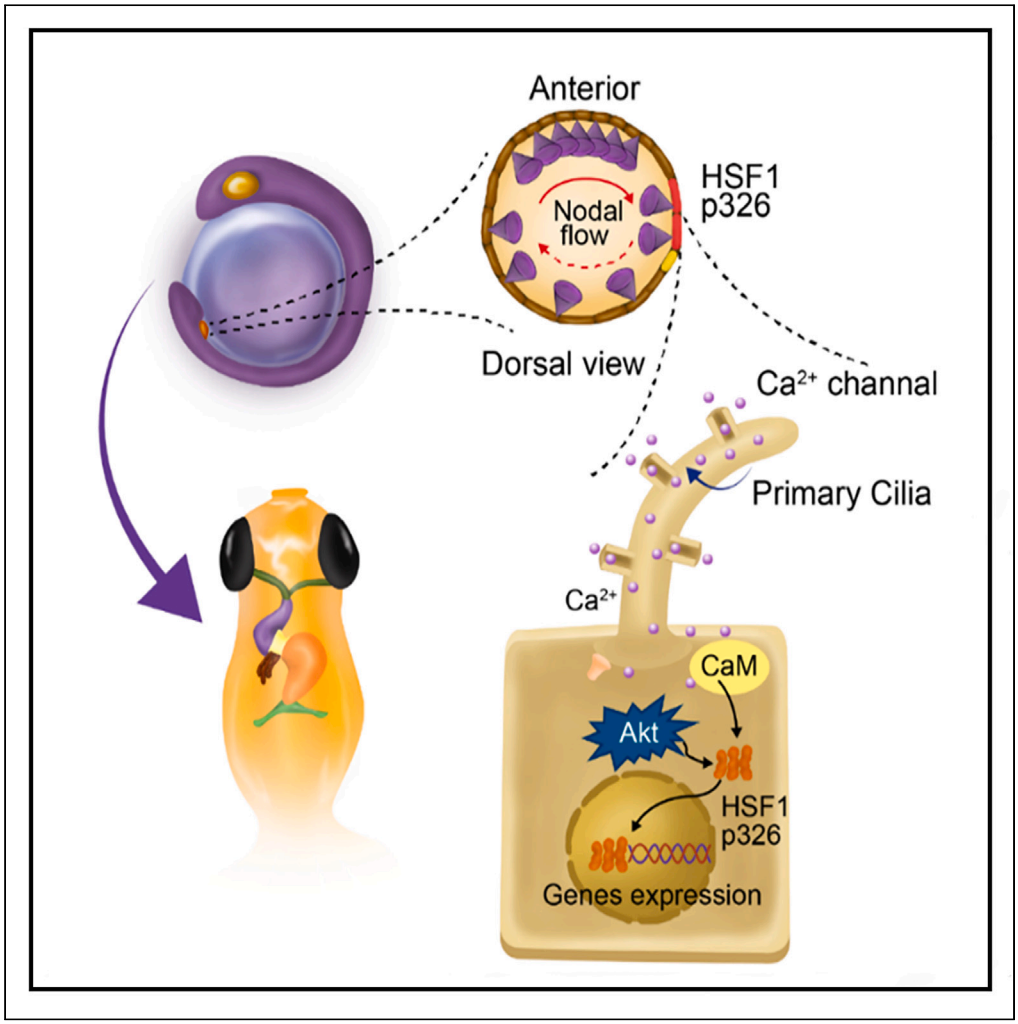

Jing Du, Shu-Kai Li, Liu-Yuan Guan, ..., Dong-Yan Chen, Hiroyuki Takeda, Yu-Bo Fan

dujing@buaa.edu.cn (J.D.)
chendy@nankai.edu.cn (D.-Y.C.)
htakeda@bs.s.u-tokyo.ac.jp (H.T.)
yubofan@buaa.edu.cn (Y.-B.F.)

Highlights

HSF1 is a mechanosensitive protein

HSF1 is a key regulator of left-right symmetry breaking

Ca^{2+}-Akt axis are essential for the activation of HSF1 under mechanical stress

Mechanical transduction is critical to embryonic development

Du et al., iScience *26*, 107864
October 20, 2023
https://doi.org/10.1016/j.isci.2023.107864

iScience

CellPress
OPEN ACCESS

Article

Mechanically sensitive HSF1 is a key regulator of left-right symmetry breaking in zebrafish embryos

Jing Du,[1,2,3,7,8,*] Shu-Kai Li,[1,7] Liu-Yuan Guan,[2,7] Zheng Guo,[1] Jiang-Fan Yin,[5] Li Gao,[5] Toru Kawanishi,[3] Atsuko Shimada,[3] Qiu-Ping Zhang,[4] Li-Sha Zheng,[1] Yi-Yao Liu,[6] Xi-Qiao Feng,[2] Lin Zhao,[4] Dong-Yan Chen,[4,*] Hiroyuki Takeda,[3,*] and Yu-Bo Fan[1,*]

SUMMARY

The left-right symmetry breaking of vertebrate embryos requires nodal flow. However, the molecular mechanisms that mediate the asymmetric gene expression regulation under nodal flow remain elusive. Here, we report that heat shock factor 1 (HSF1) is asymmetrically activated in the Kupffer's vesicle of zebrafish embryos in the presence of nodal flow. Deficiency in HSF1 expression caused a significant *situs inversus* and disrupted gene expression asymmetry of nodal signaling proteins in zebrafish embryos. Further studies demonstrated that HSF1 is a mechanosensitive protein. The mechanical sensation ability of HSF1 is conserved in a variety of mechanical stimuli in different cell types. Moreover, cilia and Ca^{2+}-Akt signaling axis are essential for the activation of HSF1 under mechanical stress *in vitro* and *in vivo*. Considering the conserved expression of HSF1 in organisms, these findings unveil a fundamental mechanism of gene expression regulation by mechanical clues during embryonic development and other physiological and pathological transformations.

INTRODUCTION

Biological flow is necessary for vertebrate organogenesis, neuron migration, cardiovascular development, and left-right (LR) symmetry breaking during embryogenesis.[1] In vertebrates, the surface of the body is symmetrical, but the internal organs and tissues are asymmetrical. Such a development process is regulated by left-right organizers (LROs). The zebrafish LRO, Kupffer's vesicle (KV), is a transient, fluid-filled vesicle organ.[2,3] The rotation of primary cilia in KV produces counterclockwise directional nodal flow, which is necessary and sufficient for breaking LR symmetry.[4,5] In KV, how the organism perceives nodal flow and the mechanism of symmetry breaking regulation are yet unclear. Two possibilities have been proposed: the chemical and mechanical senses of cilia.[6] In the ciliary chemosensory hypothesis, nodal flow may carry a morphogen, a signaling molecule, which is released into the flow and is accepted by the cilia's chemosensing function.[7] On the left and right sides of KV, the difference in the morphogen concentration detected by the receptor should be the determinant to destroy the LR symmetry. To date, however, no such morphogen has been detected, although previous studies have demonstrated the presence of chemical sensations in motile cilia.[8] On the other hand, the mechanosensory cilia that can sense the flow of fluid are involved in the occurrence of polycystic kidney disease.[9] Moreover, the nodal flow velocities on the left and right sides of zebrafish KV are not the same.[10,11] This finding indicates the possibility for the mechanical regulation function of cilia in the LR symmetry breaking. However, it remains unclear how the difference in the mechanical microenvironment in KV is sensed by cilia and transduced into gene expression regulation. In the LR organizers, mechanical and chemical senses are not necessarily mutually exclusive and but most likely coupled in a synergistic manner in zebrafish embryos. Although several signal molecules, such as Ca^{2+} and β-catenin, play important roles in the development of LR asymmetry,[12,13] the signal transduction mechanisms mediating nodal flow to gene expression regulation are largely unknown.

Regarding to gene transcriptional regulation, the heat shock protein (HSP) family of molecular chaperones shows a rapid and large transcriptional increase in response to diverse stresses, such as thermal and oxidative stress, indicating that these proteins are part of a

[1]Key Laboratory for Biomechanics and Mechanobiology of Ministry of Education, Beijing Advanced Innovation Center for Biomedical Engineering, School of Biological Science and Medical Engineering, Beihang University, Beijing 100083, China
[2]Institute of Biomechanics and Medical Engineering, Department of Mechanical Engineering, School of Aerospace, Tsinghua University, Beijing 100084, China
[3]Department of Biological Sciences, Graduate School of Science, University of Tokyo, Tokyo 113-0033, Japan
[4]Tianjin Key Laboratory of Tumor Microenvironment and Neurovascular Regulation, Department of Histology and Embryology, School of Medicine, Nankai University, Tianjin 300071, China
[5]College of life science, Hebei Normal University, Shijiazhuang 050024, China
[6]Department of Biophysics, School of Life Science and Technology, University of Electronic Science and Technology of China, Chengdu 610054, China
[7]These authors contributed equally
[8]Lead contact
*Correspondence: dujing@buaa.edu.cn (J.D.), chendy@nankai.edu.cn (D.-Y.C.), htakeda@bs.s.u-tokyo.ac.jp (H.T.), yubofan@buaa.edu.cn (Y.-B.F.)
https://doi.org/10.1016/j.isci.2023.107864

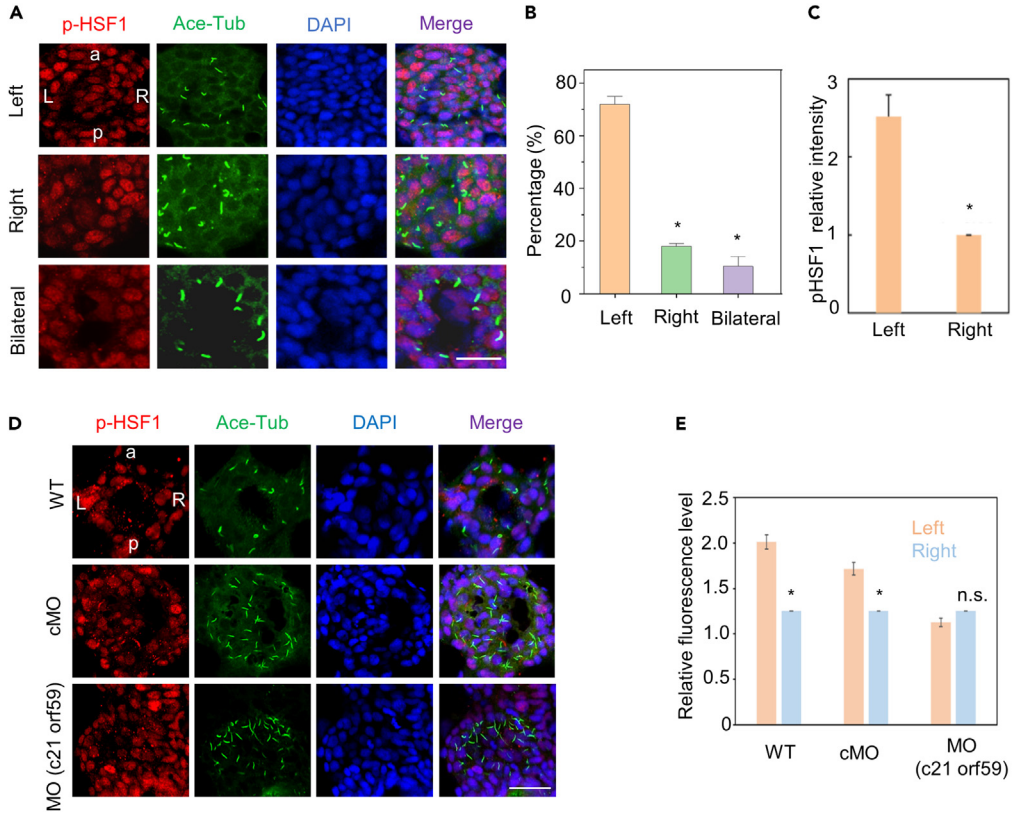

Figure 1. HSF1 is asymmetrically activated in KV of zebrafish embryos

(A) Immunostaining of phosphorylated HSF1 at serine 326 as classified by the expression pattern of left/right ratio (>1: left, <1: right, ~1: bilateral) in KV of zebrafish embryos at 8-somite stage. Cilia is indicated by acetylated α-tubulin. a: anterior, p: posterior, L: left, R: right. Scale bar: 20 μm.

(B) Statistical analysis of the percentage for three groups in (A), n = 3 from 56 embryos. Data are expressed as mean ± SEM, $p < 0.05$.

(C) Statistical analysis of the expression of pS326 HSF1 in the left and right part of KV in the case of left/right ratio >1, n = 5. Data are expressed as mean ± SEM, $p < 0.05$.

(D) Immunostaining of wild-type zebrafish embryos (WT) or embryos treated with c21orf59 MO or control morpholino (cMO). Scale bar: 25 μm.

(E) Statistical analysis of the expression level of pS326 HSF1 in the left and right part of KV in (D) (n = 4). Data are expressed as mean ± SEM, $p < 0.05$.

fundamental defense against stresses.[14–16] The master regulator of the heat shock response is heat shock factor 1 (HSF1), the key transcriptional activator of HSPs.[16] HSF1 is a highly conserved transcription factor in organisms. In addition to HSPs, HSF1 also regulates (induces or represses) the expression of other genes involved in a wide range of cellular behaviors, including apoptosis, protein trafficking, and energy generation.[17–20] Notably, the expression of FOS and JUN, two famous and well-characterized immediate-early genes, is induced in heat-shocked cells by HSF1.[21,22] Thus, the rapid activation of HSF1 has served as a model for immediate transcriptional responses and has fostered many ground-breaking insights into the regulatory mechanisms of gene expression.

In this paper, the function of HSF1 in the LR symmetry breaking process under nodal flow was addressed in zebrafish embryos. By combining *in vivo* and *in vitro* experiments, we found that HSF1 was mechanically sensitive and immediately activated by fluid shear stress and other types of mechanical stimuli though cilia, which was pivotal for the LR axis establishment during zebrafish embryonic development.

RESULTS

HSF1 is asymmetrically activated in Kupffer's vesicle of zebrafish embryos

Given that HSF1 is widely expressed throughout the early development of zebrafish embryos and conversely responds to acute stresses such as heat shock stress,[23,24] we examined the expression and activity of HSF1 in KV during LR axis determination of zebrafish embryos. As the hallmark of HSF1 activation,[25] phosphorylation level of HSF1 at serine 326 was stained in KV of 8-somite stage embryos after experimentally verifying the specificity of anti-phospho HSF1 antibody in zebrafish (Figure S1). We analyzed the expression pattern of *p*-HSF1 images according to the intensity of left/right ratio (>1: left, <1: right, ~1: bilateral). The majority of the embryos showed left-biased expression of *p*-HSF1 (left/right ratio >1 in more than 72% embryos) (Figures 1A–1C). To investigate the requirement of nodal flow in the left-biased activation of HSF1 in KV, the c21orf59 gene was knocked down using a morpholino (MO), which impaired cilia mobility and disrupted nodal flow.[26] The

A

	Genotype	Normal (%)	Reversed (%)	n
Global knockdown	Wild type	92	8	151
	hsf1 cMO	86	14	63
	hsf1 MO	48	52	66
	hsf1MO +mRNA	67	33	81
DFC specific knockdown	Control	81	19	64
	hsf1 MO	73	27	90

B

Genotype	Normal (%)	Reversed (%)	n
Widetype ($hsf1^{+/+}$)	81	19	54
heterozygote ($hsf1^{+/-}$)	83	17	41
homozygote ($hsf1^{-/-}$)	42	58	31

Figure 2. HSF1 is required for the LR asymmetry establishment of zebrafish embryos

(A) The effect of hsf1 knockdown by morpholino (MO) injection on the LR asymmetry establishment in zebrafish embryos.

(B) The effect of CRISPR/Cas9-mediated knockout of hsf1 on the LR asymmetry establishment in zebrafish embryos.

results showed that compared with WT and control morpholino embryos, c21orf59 morphants showed comparable HSF1 activity between the left and right sides of KV (Figures 1D and 1E), indicating that the asymmetric activation of HSF1 is dependent on nodal flow. These observations suggest that HSF1 is asymmetrically activated in the KV of zebrafish embryos under the action of nodal flow.

HSF1 is required for the establishment of LR asymmetry in zebrafish embryos

Considering the important roles of HSF1 in gene expression regulation, we sought to evaluate the function of HSF1 in the LR axis establishment of zebrafish embryos and gene expression patterning asymmetry in KV. Morpholino knockdown was performed to inhibit the expression of HSF1. As shown in Figure 2A, injection of HSF1 morpholino into zebrafish embryos at the one- to eight-cell stage resulted in a severely randomized localization of viscera (indicated by cardiac primordia, 52% of the HSF1 MO and 8% of control MO). The effect of HSF1 MO was further confirmed by CRISPR/Cas9-mediated knockout of hsf1, which caused 3-fold embryo ratios showing *situs inversus* in $hsf1^{-/-}$ mutants compared with WT embryos (Figure 2B). Given that KV is formed from dorsal forerunner cells (DFCs), HSF1 MO was injected into DFCs at the 50% epiboly stage to specifically inhibit the expression of HSF1 in KV. As shown in Figure 2A, DFC injection of MO also resulted in a significant *situs inversus*.

It is believed that the LR axis determination of zebrafish embryos is mediated by Nodal signals.[27] We found that knockdown of HSF1 caused severe disruption of the asymmetric expression of the nodal signaling proteins Spaw and Charon, indicating that asymmetrically activated HSF1 is an early event and could regulate nodal signals during LR axis establishment (Figures S2A–S2F). Taken together, these results suggest that HSF1 is asymmetrically activated in KV under nodal flow and plays crucial roles in LR symmetry breaking during zebrafish embryonic development.

Fluid shear stress immediately activates HSF1

As aforementioned, the effect of nodal flow could be mediated by chemical and/or mechanical sensory pathways. Recently, the heat shock response was reported to be induced by compressive loading in bovine caudal disc organ culture.[28] In addition, synovial cells stimulated by fluid shear initiate a heat shock response.[29] In rat cardiac vascular endothelial cells, stretch-sensitive ion channels regulate the activity of HSF1.[30] These studies indicate the possible function of the heat shock response in mechanical stress sensation. Thus, we investigated whether HSF1 activation in the presence of nodal flow is due to mechanical sensation of fluid shear stress. Madin-Darby canine kidney (MDCK) cells, an epithelial cell line originating from the distal renal tubular segment, were subjected to flow shear stress using a flow chamber device for cell culture to mimic fluid shear stress[31,32] (Figure 3A). Western blot experiments demonstrated that fluid shear stress induced a significant increase in HSF1 phosphorylation on the positive regulatory serine 326 reside[33] (Figures 3B and 3C). In addition, a heat shock element (HSE)-driving luciferase reporter gene (HSE-Luc) assay also demonstrated elevated transcriptional regulatory activity of HSF1 after fluid shear stress stimuli (Figure 3D).

To assess the function of cilia in the activation of HSF1 by fluid shear stress, we compared the nuclear transport of HSF1 by immunofluorescence staining in MDCK in the presence or absence of cilia. HSF1 nuclear transport was more obvious in cells with cilia than in those without

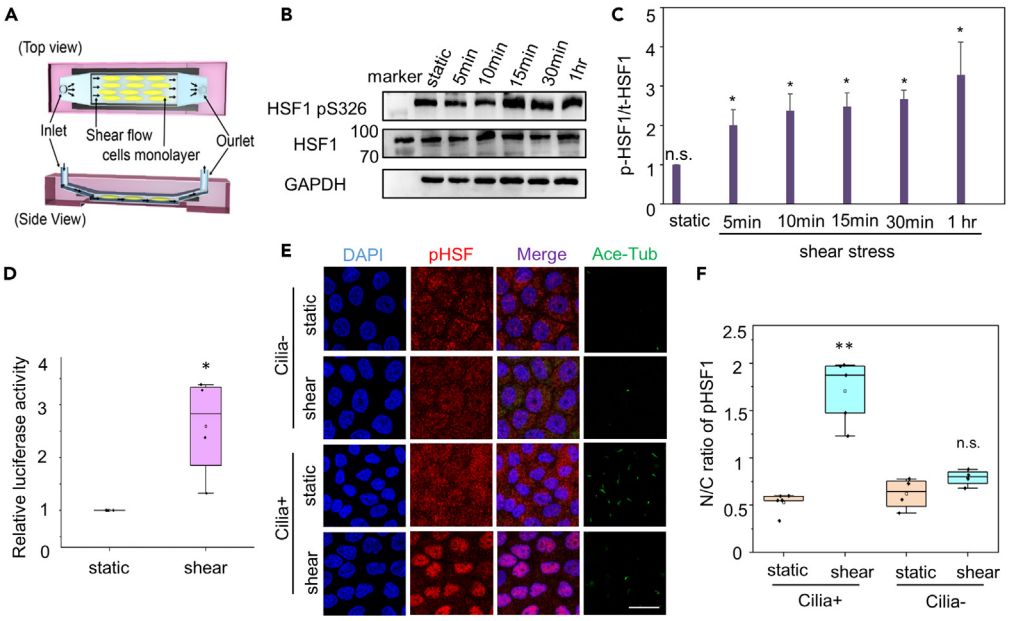

Figure 3. Immediate activation of HSF1 by fluid shear stress

(A) The illustration of the flow chamber device for fluid shear stress experiments.

(B) Western blot results of phosphorylated HSF1 at Serine 326 or 303 in MDCK cells after shear stress stimuli for different time.

(C) Statistical analysis of the results in (B) (n = 3). The ratio of phosphorylated HSF1 at Serine 326 in nuclei and cytoplasm (N/C) in (B) (n = 10). Data are expressed as mean ± SEM, p<0.05.

(D) Luciferase reporter assay for HSE activity in MDCK cells treated with shear stress for 1 h. (n = 3). Data are expressed as mean ± SEM, p < 0.05.

(E) Fluorescent immunostaining of phosphorylated HSF1 at Serine 326 in MDCK cells 30 min after shear stress. Scale bar: 25 μm.

(F) The ratio of phosphorylated HSF1 at Serine 326 in nuclei and cytoplasm (N/C) in (E). Data are expressed as mean ± SEM, p < 0.01.

cilia, indicating the contribution of cilia to the activation of HSF1 under fluid shear stress (Figures 3E and 3F). These observations are consistent with the mechanical sensing function of cilia, which has been reported in different cell types.[34]

Mechanical sensitivity of HSF1 is conserved in various types of mechanical stimuli

Next, to evaluate the versatility of HSF1 in mechanical sensing, other types of mechanical stimuli were applied to MDCK cells, including mechanical stretch, hypergravity, and substrate stiffness. As shown in Figures S3 and S4, mechanical stretch and hypergravity stimuli also triggered rapid nuclear transportation of HSF1 and a significant increase in hsp70 gene expression. Moreover, HSF1 activity was also regulated by substrate stiffness. Compared to the compliant substrate (0.5 kPa), adhesion to the stiff substrate (500 kPa) significantly induced immediate nuclear transportation of HSF1 (Figure 4). To evaluate the conservation of the mechanical sensing function of HSF1 in different cell types, we examined the activation of HSF1 by substrate stiffness in mesenchymal stem cells (MSCs), which are generally used as a cell model for mechanical sensing research.[35,36] The results demonstrated rapid nuclear transportation of HSF1 in MSCs on stiff substrates, which was not observed on soft substrates (Figure S5). Collectively, these results suggest that HSF1 is a versatile mechanosensor that can immediately transduce extracellular mechanical stress to gene transcriptional regulation in cells.

Mechanical shear stress activates HSF1 mainly through the Ca^{2+}-Akt signaling axis

To investigate the molecular mechanism underlying HSF1 activation triggered by mechanical stress, we screened signaling pathways that are generally evidenced as important mediators in extracellular signal transduction, including MEK, MAPK, Akt, PKC, and CaMKII.[37–41] The results showed that HSF1 activation under fluid shear stress was strikingly blocked by the Akt inhibitor, whereas a moderate decrease in HSF1 activity was observed in the presence of MAPK, MEK, CaMKII, or PKC inhibitors (Figures 5A and 5B). These results were consistent with a previous report that Akt could directly interact with HSF1 and phosphorylate it at the positive regulatory residue serine 326.[42]

Many studies have demonstrated that fluid shear stress stimulation induces rapid and temporal intracellular Ca^{2+} increases in many cell types, including MDCK.[43–46] Moreover, Ca^{2+} has a crucial effect on Akt signaling in various cell types.[47–50] Thus, Ca^{2+} signaling may be an upstream signal involved in the immediate activation of HSF1 by mechanical shear stress. To assess this hypothesis, intracellular Ca^{2+} was inhibited by the membrane-permeable Ca^{2+} chelator BAPTA-AM or promoted by additional treatment with Ca^{2+} in the presence of fluid shear stress stimuli. As shown in Figures 5C–5E, BAPTA-AM dramatically blocked fluid shear stress-induced HSF1 activation, which could be rescued by excess Ca^{2+}. Moreover, additional Ca^{2+} synergistically upregulated HSF1 activity together with fluid shear stress. These results indicate that rapid activation of HSF1 by mechanical stress is mainly mediated by Ca^{2+}-Akt signaling pathway.

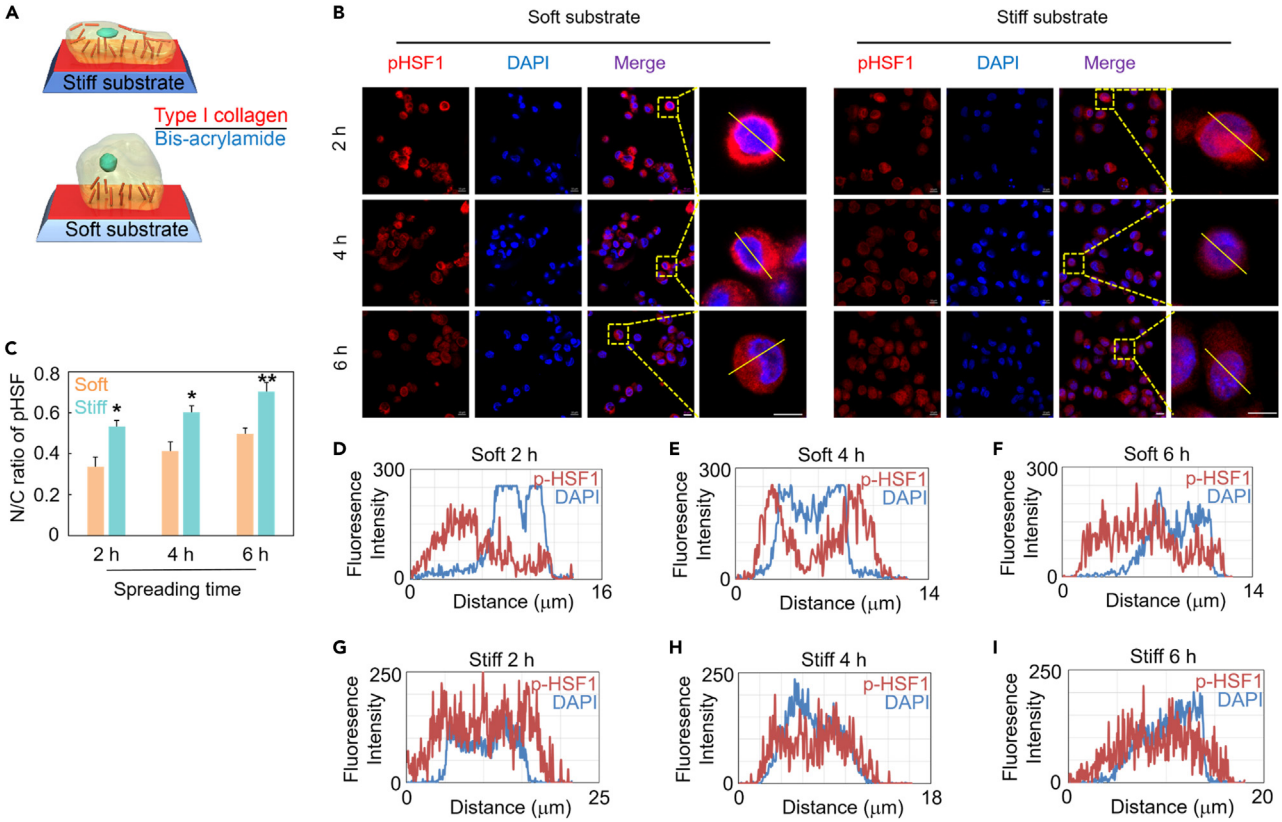

Figure 4. HSF1 activity was regulated by substrate stiffness

(A) The illustration of the experiment device for substrate stiffness stimuli to cultured cells.

(B) Fluorescent immunostaining of phosphorylated HSF1 at Serine 326 in MDCK cells under substrate stiffness stimuli. Scale bar: 10 μm.

(C) The ratio of phosphorylated HSF1 at Serine 326 in nuclei and cytoplasm (N/C) in (B) (n = 9). Data are expressed as mean ± SEM, *p < 0.05, **p < 0.01.

(D–I) Fluorescence intensity of phosphorylated HSF1 at Serine 326 and DAPI along the lines in the magnified figures in (B).

During zebrafish embryonic development, it has been reported that the left-biased Ca^{2+} concentration in KV plays a vital role in LR symmetry breaking.[12,13] In the aforementioned study, we found that Ca^{2+} signaling was crucial for the rapid activation of HSF1 induced by fluid shear stress. To assess whether the left-biased activation of HSF1 in KV also requires Ca^{2+} signaling, we treated zebrafish embryos with an inhibitor of the endoplasmic reticulum Ca-ATPase (thapsigargin, TG) to deplete intracellular Ca^{2+} stores. As shown in Figures 6A and 6B, the asymmetrical activation of HSF1 was largely blocked by inhibition of Ca^{2+}. Further, we treated embryos with an Akt inhibitor (MK-2206), which has been reported to block Akt signaling pathway in zebrafish.[51] The results showed a significant downregulation of left-biased activation of HSF1 by Akt inhibition (Figures 6C and 6D). These results suggest that Ca^{2+}-Akt signaling axis is essential for the activation of HSF1 in KV. Thus, we propose a model in which the left-biased activation of HSF1 in KV transduces the mechanical shear stress of nodal flow into gene transcriptional regulation in the dependence of Ca^{2+} signal during LR axis establishment of zebrafish embryos.

DISCUSSION

Quite a few hypotheses regarding how KV perceives symmetry and regulates symmetry destruction have been proposed in the previous studies, including that cilia perceive the mechanical signal of fluid flow.[34,52] Many studies have shown that the distribution of cilia is not uniform and that the flow velocity of the fluid in the cavity caused by cilia is not the same.[10] This makes the mechanical environment in KV different, which provides the possibility for the destruction of KV symmetry caused by cilia sensing the mechanical stimulus. Assuming that the cilia on the left and right sides of the KV produce asymmetric signals, the signal cascade will be initiated, which will lead to asymmetric gene expression. However, this mechanical sensing hypothesis lacks a pivotal mechanism for how the difference in the mechanical microenvironment in KV is transduced into gene expression regulation.

In our experiments, we found that hsf1 and hsf2 mRNA expressions were both observed at the 5–8 somite stage (Figure S6A). As shown in Figure S6B, HSF2 inhibition also affected LR axis determination. However, the effect of HSF2 morpholino was not obvious compared to HSF1 inhibition (Figure 2A). Therefore, we mainly assessed the role of HSF1 in the LR symmetry breaking in this study. In future studies, more experiments, such as double mutants, should be conducted in order to evaluate whether there is a compensating effect of HSF2 in HSF1 mutant

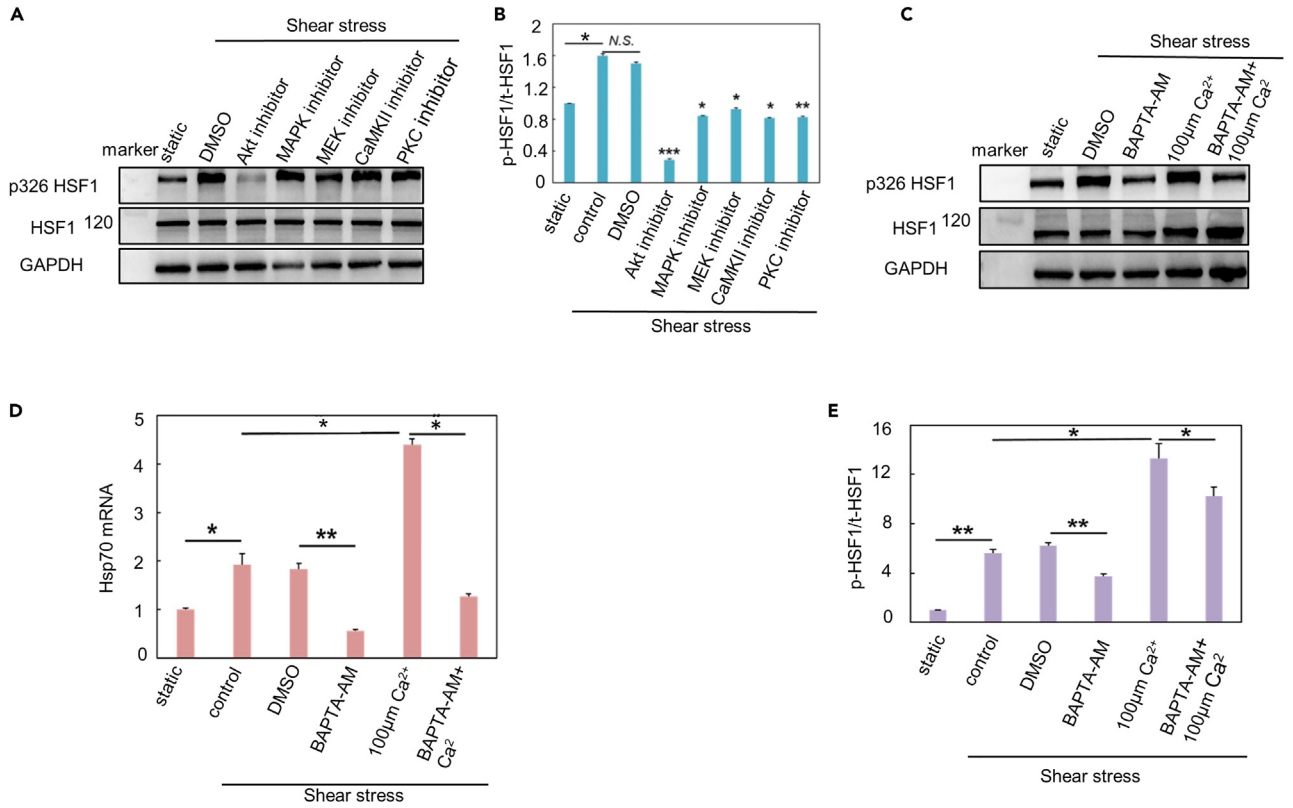

Figure 5. Ca^{2+} and Akt signals were involved in HSF1 activation by shear stress

(A) Western blot results of phosphorylated HSF1 at serine 326 and total HSF1 in MDCK cells under shear stress in the presence of inhibitors or DMSO.

(B) Statistical analysis of the results in (A) (n = 3). Data are expressed as mean ± SEM, *p < 0.05, **p < 0.01,***p < 0.001 (C) Western blot results of phosphorylated HSF1 at serine 326 and total HSF1 in MDCK cells under shear stress in the presence of Ca2+ antagonist or Ca2+.

(D) Statistical analysis of the results in (B) (n = 3). Data are expressed as mean ± SEM, *p < 0.05, **p < 0.01.

(E) The expression level of hsp70 mRNA in MDCK cells under shear stress in the presence of Ca^{2+} antagonist or Ca^{2+} (n = 3). Data are expressed as mean ± SEM, *p < 0.05, **p < 0.01.

to affect the LR symmetry breaking of zebrafish embryos. We demonstrated that HSF1 is sensitive to fluid shear stress and immediately transduces mechanical stimuli into gene transcriptional regulation. Thus, our findings support the important role of mechanical conduction in the mechanism of LR symmetry breaking during zebrafish development. According to our results, HSF1 activation is dependent on the cilia, which further confirms the function of cilia in sensing nodal flow.

Although HSF1 has previously been linked to cilia motility in postnatal HSF1-null mice,[53] we observed normal cilia beating in KV after HSF1 knockdown by morpholino in zebrafish. Moreover, microinjected of fluorescent particles into the KV lumen also showed leftward fluid flow in HSF1 morphants and WT embryos (Videos S1, S2, and S3). These results indicate the possible role of mechanical sensing by HSF1 in L-R patterning of zebrafish embryo. During zebrafish embryonic development, charon is transiently right-biased expressed in the regions embracing KV at the 8–10 somite stage, which is required for LR patterning.[54–57] Miss-expression of charon elicited phenotypes similar to those of mutant embryos defective in Nodal signaling, which resulted in a loss of LR polarity. We found that HSF1 was asymmetrically activated in KV as early as 8 somite states, and injection of HSF1 MO led to a randomized expression of charon and spaw. Thus, asymmetrical activation of HSF1 may be a relatively early event during LR axis determination. Moreover, using bioinformatics analysis, we found several HSEs in the promoter region of zebrafish charon gene (Figure S7). Thus, we hypothesize that HSF1 may contribute to the regulation of charon expression during LR axis establishment.

In the response to mechanical stimuli by cells, mechanical signals must be transduced into the nuclei to influence gene expression. Thus, the responses of cells to external mechanical stimuli are time-dependent. However, the time effect of mechanical transduction processes has not been completely studied. In this paper, we identified that HSF1, as a transcription factor, was immediately activated by mechanical stimuli and it rapidly transmitted mechanical signals into gene transcriptional regulation upon various types of mechanical stimuli. Similar to the immediate-early genes, the first round of gene transcription after stimuli should be the "gateway" of the complete mechanical response. Thus, the immediate-early activation of HSF1 by mechanical stress may be a conserved signal transduction mechanism for gene transcription regulation in the rapid response to mechanical stimuli by cells.

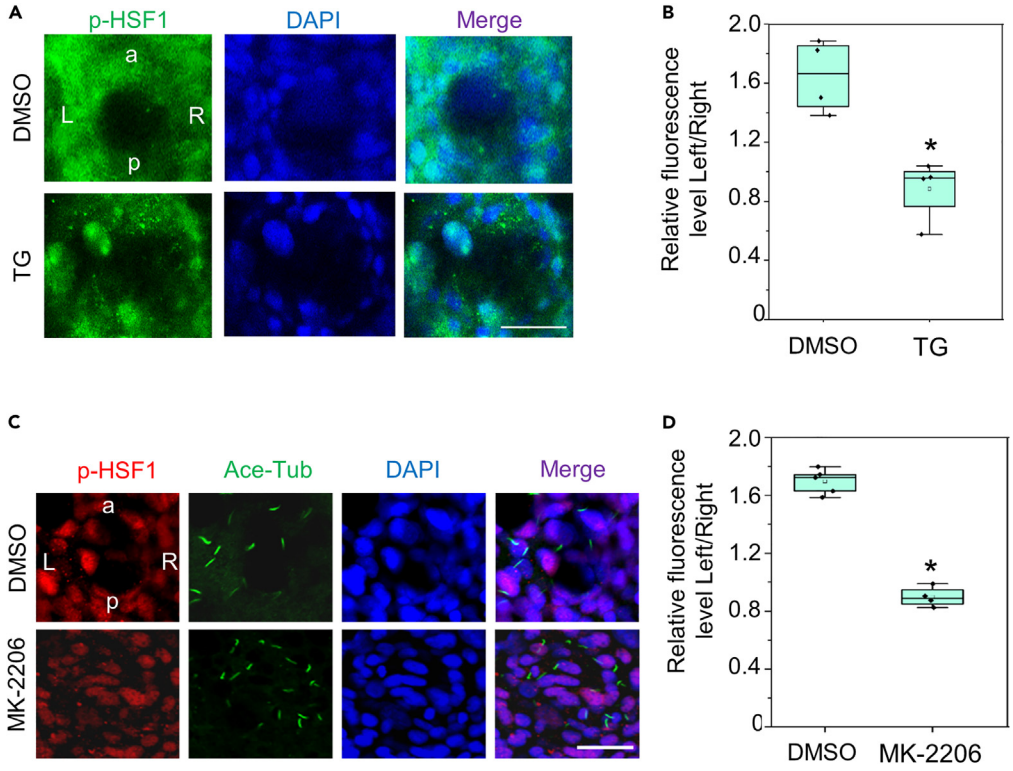

Figure 6. Ca^{2+} and Akt signals were involved in HSF1 activation *in vivo*

(A) Immunostaining of phosphorylated HSF1 at serine 326 in zebrafish embryos treated with DMSO or 1 μM thapsigargin (TG), scale bar: 25 μm.

(B) The left/right ratio of phosphorylated HSF1 at serine 326 in (A) (n = 3). Data are expressed as mean ± SEM, *p < 0.05.

(C) Immunostaining of phosphorylated HSF1 at Serine 326 in zebrafish embryos treated with DMSO or 5 μM MK-2206 (Akt inhibitor), scale bar: 25 μm.

(D) The left/right ratio of phosphorylated HSF1 at serine 326 in (C) (n = 4). Data are expressed as mean ± SEM, *p < 0.05.

The heat shock response is a fundamental defense against stress. As a highly conserved transcription factor in organisms, HSF1 regulates (induces or represses) the expression of genes that are involved in a wide range of cellular behaviors. Thus, the rapid activation of HSF1 serves as a model for immediate transcriptional responses and has fostered many ground-breaking insights into the regulatory mechanisms of gene expression. Our findings unveiled that in addition to thermal and oxidative stresses, HSF1 also responds to mechanical stresses, which is important for gene regulation triggered by mechanical clues during embryonic development and other physiological and pathological transformations.

Limitations of the study

In zebrafish experiments, we have not completely proved whether HSF2 in HSF1 mutant has a compensating effect on LR symmetry breaking. Hopefully, we will be able to supplement this part in the future by generating the maternal-zygotic double mutants.

In the paper, we identified the mechanical sensing ability of HSF1 in different cells through different mechanical stimuli, but we did not fully identify the mechanical sensing mechanism of early activation of HSF1. This makes us less specific about the effects of early mechanical transduction in organisms on embryonic development and other physiological processes. That is what we aregoing to focus on in the future, and hopefully we will be able to add to that in the future.

STAR★METHODS

Detailed methods are provided in the online version of this paper and include the following:

- KEY RESOURCES TABLE
- RESOURCE AVAILABILITY
  - Lead contact
  - Materials availability
  - Data and code availability
- EXPERIMENTAL MODEL AND STUDY PARTICIPANT DETAILS

SUPPLEMENTAL INFORMATION

Supplemental information can be found online at https://doi.org/10.1016/j.isci.2023.107864.

ACKNOWLEDGMENTS

We thank A.M. Meng (Tsinghua University) for technical assistance and discussions in the course of the preparation of this manuscript. We also thank H. Yamaguchi (The University of Tokyo) for technical assistance of zebrafish experiments. We wish to thank Dr. XunWei Xie from the China Zebrafish Resource Center for helping in the generation of geneX-mutant zebrafish. We thank Professor A.M.Meng (Tsinghua University) for technical assistance.

This work was supported by the National Natural Science Foundation of China (12222201, 82273500, 81901346, 62027812, and U20A20390) and Fundamental Research Funds for the Central Universities (ZG140S1971).

AUTHOR CONTRIBUTIONS

Y.B.F., H.T., D.Y.C., and J.D. designed the study and interpreted experiments. J.D., S.K.L., and L.Y.G performed cell and zebrafish experiments. Z.G., T.K., A.S., and Q.P.Z. helped with the zebrafish experiments. J.F.Y., L.G., L.S.Z., Y.Y.L., and X.Q.F. helped with the cell mechanical stimuli experiments. Y.B.F., H.T., D.Y.C., and J.D. conceived and supervised this project and wrote the paper.

DECLARATION OF INTERESTS

There are no competing interests.

Received: May 9, 2021
Revised: May 8, 2023
Accepted: August 30, 2023
Published: September 9, 2023

REFERENCES

1. Freund, J.B., Goetz, J.G., Hill, K.L., and Vermot, J. (2012). Fluid flows and forces in development: functions, features and biophysical principles. Development *139*, 1229–1245.
2. Essner, J.J., Amack, J.D., Nyholm, M.K., Harris, E.B., and Yost, H.J. (2005). Kupffer's vesicle is a ciliated organ of asymmetry in the zebrafish embryo that initiates left-right development of the brain, heart and gut. Development *132*, 1247–1260. https://doi.org/10.1242/dev.01663.
3. Kramer-Zucker, A.G., Olale, F., Haycraft, C.J., Yoder, B.K., Schier, A.F., and Drummond, I.A. (2005). Cilia-driven fluid flow in the zebrafish pronephros, brain and Kupffer's vesicle is required for normal organogenesis. Development *132*, 1907–1921. https://doi.org/10.1242/dev.01772.
4. Hojo, M., Takashima, S., Kobayashi, D., Sumeragi, A., Shimada, A., Tsukahara, T., Yokoi, H., Narita, T., Jindo, T., Kage, T., et al. (2007). Right-elevated expression of charon is regulated by fluid flow in medaka Kupffer's vesicle. Dev. Growth Differ. *49*, 395–405.
5. Kreiling, J.A., Prabhat, Williams, G., and Creton, R. (2007). Analysis of Kupffer's vesicle in zebrafish embryos using a cave automated virtual environment. Dev. Dyn. *236*, 1963–1969.
6. Tabin, C.J., and Vogan, K.J. (2003). A two-cilia model for vertebrate left-right axis specification. Genes Dev. *17*, 1–6. https://doi.org/10.1101/gad.1053803.
7. Cartwright, J.H.E., Piro, O., and Tuval, I. (2004). Fluid-dynamical basis of the embryonic development of left-right asymmetry in vertebrates. Proc. Natl. Acad. Sci. USA *101*, 7234–7239. https://doi.org/10.1073/pnas.0402001101.
8. Shah, A.S., Ben-Shahar, Y., Moninger, T.O., Kline, J.N., and Welsh, M.J. (2009). Motile cilia of human airway epithelia are chemosensory. Science *325*, 1131–1134. https://doi.org/10.1126/science.1173869.
9. Yoder, B.K. (2007). Role of primary cilia in the pathogenesis of polycystic kidney disease. J. Am. Soc. Nephrol. *18*, 1381–1388. https://doi.org/10.1681/ASN.2006111215.
10. Montenegro-Johnson, T.D., Baker, D.I., Smith, D.J., and Lopes, S.S. (2016). Three-dimensional flow in Kupffer's Vesicle. J. Math.

Biol. *73*, 705–725. https://doi.org/10.1007/s00285-016-0967-7.

11. Sampaio, P., Ferreira, R.R., Guerrero, A., Pintado, P., Tavares, B., Amaro, J., Smith, A.A., Montenegro-Johnson, T., Smith, D.J., and Lopes, S.S. (2014). Left-right organizer flow dynamics: how much cilia activity reliably yields laterality? Dev. Cell *29*, 716–728. https://doi.org/10.1016/j.devcel.2014.04.030.
12. Yuan, S., Zhao, L., Brueckner, M., and Sun, Z. (2015). Intraciliary calcium oscillations initiate vertebrate left-right asymmetry. Curr. Biol. *25*, 556–567.
13. Takao, D., Nemoto, T., Abe, T., Kiyonari, H., Kajiura-Kobayashi, H., Shiratori, H., and Nonaka, S. (2013). Asymmetric distribution of dynamic calcium signals in the node of mouse embryo during left–right axis formation. Dev. Biol. *376*, 23–30.
14. Voellmy, R., and Boellmann, F. (2007). Chaperone regulation of the heat shock protein response. In Molecular Aspects of the Stress Response: Chaperones, Membranes and Networks (Springer), pp. 89–99.
15. Vígh, L., Török, Z., Balogh, G., Glatz, A., Piotto, S., and Horváth, I. (2007). Membrane-regulated stress response. In Molecular Aspects of the Stress Response: Chaperones, Membranes and Networks (Springer), pp. 114–131.
16. Ryno, L.M., Genereux, J.C., Naito, T., Morimoto, R.I., Powers, E.T., Shoulders, M.D., and Wiseman, R.L. (2014). Characterizing the altered cellular proteome induced by the stress-independent activation of heat shock factor 1. ACS Chem. Biol. *9*, 1273–1283.
17. Kus-Liśkiewicz, M., Polańska, J., Korfanty, J., Olbryt, M., Vydra, N., Toma, A., and Widłak, W. (2013). Impact of heat shock transcription factor 1 on global gene expression profiles in cells which induce either cytoprotective or pro-apoptotic response following hyperthermia. BMC Genom. *14*, 456. https://doi.org/10.1186/1471-2164-14-456.
18. Hahn, J.S., Hu, Z., Thiele, D.J., and Iyer, V.R. (2004). Genome-wide analysis of the biology of stress responses through heat shock transcription factor. Mol. Cell Biol. *24*, 5249–5256. https://doi.org/10.1128/MCB.24.12.5249-5256.2004.
19. Page, T.J., Sikder, D., Yang, L., Pluta, L., Wolfinger, R.D., Kodadek, T., and Thomas, R.S. (2006). Genome-wide analysis of human HSF1 signaling reveals a transcriptional program linked to cellular adaptation and survival. Mol. Biosyst. *2*, 627–639. https://doi.org/10.1039/b606129j.
20. Birch-Machin, I., Gao, S., Huen, D., McGirr, R., White, R.A.H., and Russell, S. (2005). Genomic analysis of heat-shock factor targets in Drosophila. Genome Biol. *6*, R63. https://doi.org/10.1186/gb-2005-6-7-r63.
21. Ishikawa, T., Igarashi, T., Hata, K., and Fujita, T. (1999). c-fos induction by heat, arsenite, and cadmium is mediated by a heat shock element in its promoter. Biochem. Biophys. Res. Commun. *254*, 566–571. https://doi.org/10.1006/bbrc.1998.9979.
22. Sawai, M., Ishikawa, Y., Ota, A., and Sakurai, H. (2013). The proto-oncogene JUN is a target of the heat shock transcription factor HSF1. FEBS J. *280*, 6672–6680. https://doi.org/10.1111/febs.12570.
23. Wang, G., Huang, H., Dai, R., Lee, K.Y., Lin, S., and Mivechi, N.F. (2001). Suppression of heat shock transcription factor HSF1 in zebrafish causes heat-induced apoptosis. Genesis *30*, 195–197.
24. Evans, T.G., Belak, Z., Ovsenek, N., and Krone, P.H. (2007). Heat shock factor 1 is required for constitutive Hsp70 expression and normal lens development in embryonic zebrafish. Comp. Biochem. Physiol. Mol. Integr. Physiol. *146*, 131–140. https://doi.org/10.1016/j.cbpa.2006.09.023.
25. Chou, S.D., Prince, T., Gong, J., and Calderwood, S.K. (2012). mTOR is essential for the proteotoxic stress response, HSF1 activation and heat shock protein synthesis. PLoS One *7*, e39679. https://doi.org/10.1371/journal.pone.0039679.
26. Jaffe, K.M., Grimes, D.T., Schottenfeld-Roames, J., Werner, M.E., Ku, T.S.J., Kim, S.K., Pelliccia, J.L., Morante, N.F.C., Mitchell, B.J., and Burdine, R.D. (2016). c21orf59/kurly Controls Both Cilia Motility and Polarization. Cell Rep. *14*, 1841–1849. https://doi.org/10.1016/j.celrep.2016.01.069.
27. Koshida, S., Shinya, M., Mizuno, T., Kuroiwa, A., and Takeda, H. (1998). Initial anteroposterior pattern of the zebrafish central nervous system is determined by differential competence of the epiblast. Development *125*, 1957–1966.
28. Chooi, W.H., Chan, S.C.W., Gantenbein, B., and Chan, B.P. (2016). Loading-Induced Heat-Shock Response in Bovine Intervertebral Disc Organ Culture. PLoS One *11*, e0161615. https://doi.org/10.1371/journal.pone.0161615.
29. Schett, G., Redlich, K., Xu, Q., Bizan, P., Gröger, M., Tohidast-Akrad, M., Kiener, H., Smolen, J., and Steiner, G. (1998). Enhanced expression of heat shock protein 70 (hsp70) and heat shock factor 1 (HSF1) activation in rheumatoid arthritis synovial tissue. Differential regulation of hsp70 expression and hsf1 activation in synovial fibroblasts by proinflammatory cytokines, shear stress, and antiinflammatory drugs. J. Clin. Invest. *102*, 302–311. https://doi.org/10.1172/JCI2465.
30. Chang, J., Wasser, J.S., Cornelussen, R.N., and Knowlton, A.A. (2001). Activation of heat-shock factor by stretch-activated channels in rat hearts. Circulation *104*, 209–214.
31. Duan, Y., Weinstein, A.M., Weinbaum, S., and Wang, T. (2010). Shear stress-induced changes of membrane transporter localization and expression in mouse proximal tubule cells. Proc. Natl. Acad. Sci. USA *107*, 21860–21865. https://doi.org/10.1073/pnas.1015751107.
32. Tarran, R., Button, B., Picher, M., Paradiso, A.M., Ribeiro, C.M., Lazarowski, E.R., Zhang, L., Collins, P.L., Pickles, R.J., Fredberg, J.J., and Boucher, R.C. (2005). Normal and cystic fibrosis airway surface liquid homeostasis. The effects of phasic shear stress and viral infections. J. Biol. Chem. *280*, 35751–35759. https://doi.org/10.1074/jbc.M505832200.
33. Guettouche, T., Boellmann, F., Lane, W.S., and Voellmy, R. (2005). Analysis of phosphorylation of human heat shock factor 1 in cells experiencing a stress. BMC Biochem. *6*, 4. https://doi.org/10.1186/1471-2091-6-4.
34. R Ferreira, R., Fukui, H., Chow, R., Vilfan, A., and Vermot, J. (2019). The cilium as a force sensor-myth versus reality. J. Cell Sci. *132*, jcs213496. https://doi.org/10.1242/jcs.213496.
35. Engler, A.J., Sen, S., Sweeney, H.L., and Discher, D.E. (2006). Matrix elasticity directs stem cell lineage specification. Cell *126*, 677–689. https://doi.org/10.1016/j.cell.2006.06.044.
36. Du, J., Chen, X., Liang, X., Zhang, G., Xu, J., He, L., Zhan, Q., Feng, X.Q., Chien, S., and Yang, C. (2011). Integrin activation and internalization on soft ECM as a mechanism of induction of stem cell differentiation by ECM elasticity. Proc. Natl. Acad. Sci. USA *108*, 9466–9471. https://doi.org/10.1073/pnas.1106467108.
37. Leevers, S.J., and Marshall, C.J. (1992). Activation of extracellular signal-regulated kinase, ERK2, by p21ras oncoprotein. EMBO J. *11*, 569–574.
38. Cargnello, M., and Roux, P.P. (2011). Activation and function of the MAPKs and their substrates, the MAPK-activated protein kinases. Microbiol. Mol. Biol. Rev. *75*, 50–83. https://doi.org/10.1128/MMBR.00031-10.
39. Dudek, H., Datta, S.R., Franke, T.F., Birnbaum, M.J., Yao, R., Cooper, G.M., Segal, R.A., Kaplan, D.R., and Greenberg, M.E. (1997). Regulation of neuronal survival by the serine-threonine protein kinase Akt. Science *275*, 661–665.
40. Reyland, M.E. (2009). Protein kinase C isoforms: Multi-functional regulators of cell life and death. Front. Biosci. *14*, 2386–2399.
41. Hudmon, A., and Schulman, H. (2002). Neuronal CA2+/calmodulin-dependent protein kinase II: the role of structure and autoregulation in cellular function. Annu. Rev. Biochem. *71*, 473–510. https://doi.org/10.1146/annurev.biochem.71.110601.135410.
42. Carpenter, R.L., Paw, I., Dewhirst, M.W., and Lo, H.W. (2015). Akt phosphorylates and activates HSF-1 independent of heat shock, leading to Slug overexpression and epithelial-mesenchymal transition (EMT) of HER2-overexpressing breast cancer cells. Oncogene *34*, 546–557. https://doi.org/10.1038/onc.2013.582.
43. Praetorius, H.A., and Spring, K.R. (2001). Bending the MDCK cell primary cilium increases intracellular calcium. J. Membr. Biol. *184*, 71–79.
44. Yamamoto, K., Korenaga, R., Kamiya, A., and Ando, J. (2000). Fluid shear stress activates Ca(2+) influx into human endothelial cells via P2X4 purinoceptors. Circ. Res. *87*, 385–391.
45. Jafarnejad, M., Cromer, W.E., Kaunas, R.R., Zhang, S.L., Zawieja, D.C., and Moore, J.E., Jr. (2015). Measurement of shear stress-mediated intracellular calcium dynamics in human dermal lymphatic endothelial cells. Am. J. Physiol. Heart Circ. Physiol. *308*, H697–H706. https://doi.org/10.1152/ajpheart.00744.2014.
46. Schwarz, G., Callewaert, G., Droogmans, G., and Nilius, B. (1992). Shear stress-induced calcium transients in endothelial cells from human umbilical cord veins. J. Physiol. *458*, 527–538.
47. Danciu, T.E., Adam, R.M., Naruse, K., Freeman, M.R., and Hauschka, P.V. (2003). Calcium regulates the PI3K-Akt pathway in stretched osteoblasts. FEBS Lett. *536*, 193–197.
48. Nicholson-Fish, J.C., Cousin, M.A., and Smillie, K.J. (2016). Phosphatidylinositol 3-Kinase Couples Localised Calcium Influx to Activation of Akt in Central Nerve Terminals. Neurochem. Res. *41*, 534–543. https://doi.org/10.1007/s11064-015-1663-5.
49. Pérez-García, M.J., Ceña, V., de Pablo, Y., Llovera, M., Comella, J.X., and Soler, R.M. (2004). Glial cell line-derived neurotrophic factor increases intracellular calcium concentration. Role of calcium/calmodulin in the activation of the phosphatidylinositol 3-kinase pathway. J. Biol. Chem. *279*, 6132–6142. https://doi.org/10.1074/jbc.M308367200.

50. Divolis, G., Mavroeidi, P., Mavrofrydi, O., and Papazafiri, P. (2016). Differential effects of calcium on PI3K-Akt and HIF-1alpha survival pathways. Cell Biol. Toxicol. *32*, 437–449. https://doi.org/10.1007/s10565-016-9345-x.
51. Luo, J., Lu, C., Feng, M., Dai, L., Wang, M., Qiu, Y., Zheng, H., Liu, Y., Li, L., Tang, B., et al. (2021). Cooperation between liver-specific mutations of pten and tp53 genetically induces hepatocarcinogenesis in zebrafish. J. Exp. Clin. Cancer Res. *40*, 262. https://doi.org/10.1186/s13046-021-02061-y.
52. Omori, T., Winter, K., Shinohara, K., Hamada, H., and Ishikawa, T. (2018). Simulation of the nodal flow of mutant embryos with a small number of cilia: comparison of mechanosensing and vesicle transport hypotheses. R. Soc. Open Sci. *5*, 180601. https://doi.org/10.1098/rsos.180601.
53. Takaki, E., Fujimoto, M., Nakahari, T., Yonemura, S., Miyata, Y., Hayashida, N., Yamamoto, K., Vallee, R.B., Mikuriya, T., Sugahara, K., et al. (2007). Heat shock transcription factor 1 is required for maintenance of ciliary beating in mice. J. Biol. Chem. *282*, 37285–37292. https://doi.org/10.1074/jbc.M704562200.
54. Hojo, M., Takashima, S., Kobayashi, D., Sumeragi, A., Shimada, A., Tsukahara, T., Yokoi, H., Narita, T., Jindo, T., Kage, T., et al. (2007). Right-elevated expression of charon is regulated by fluid flow in medaka Kupffer's vesicle. Dev. Growth Differ. *49*, 395–405. https://doi.org/10.1111/j.1440-169X.2007.00937.x.
55. Schneider, I., Schneider, P.N., Derry, S.W., Lin, S., Barton, L.J., Westfall, T., and Slusarski, D.C. (2010). Zebrafish Nkd1 promotes Dvl degradation and is required for left-right patterning. Dev. Biol. *348*, 22–33. https://doi.org/10.1016/j.ydbio.2010.08.040.
56. Kawasumi, A., Nakamura, T., Iwai, N., Yashiro, K., Saijoh, Y., Belo, J.A., Shiratori, H., and Hamada, H. (2011). Left-right asymmetry in the level of active Nodal protein produced in the node is translated into left-right asymmetry in the lateral plate of mouse embryos. Dev. Biol. *353*, 321–330. https://doi.org/10.1016/j.ydbio.2011.03.009.
57. Nakamura, T., Saito, D., Kawasumi, A., Shinohara, K., Asai, Y., Takaoka, K., Dong, F., Takamatsu, A., Belo, J.A., Mochizuki, A., and Hamada, H. (2012). Fluid flow and interlinked feedback loops establish left-right asymmetric decay of Cerl2 mRNA. Nat. Commun. *3*, 1322. https://doi.org/10.1038/ncomms2319.
58. Du, J., Zu, Y., Li, J., Du, S., Xu, Y., Zhang, L., Jiang, L., Wang, Z., Chien, S., and Yang, C. (2016). Extracellular matrix stiffness dictates Wnt expression through integrin pathway. Sci. Rep. *6*, 20395. https://doi.org/10.1038/srep20395.
59. Amack, J.D., and Yost, H.J. (2004). The T box transcription factor no tail in ciliated cells controls zebrafish left-right asymmetry. Curr. Biol. *14*, 685–690. https://doi.org/10.1016/j.cub.2004.04.002.

STAR★METHODS

KEY RESOURCES TABLE

REAGENT or RESOURCE	SOURCE	IDENTIFIER
Antibodies		
Anti-HSF1	Abcam	Ab105086
Anti-HSF1 phospho S326	Abcam	ab76076
Anti-Acetylated Tubulin	Sigma	T6793
Alexa Fluor 555 goat anti-Rabbit secondary polyclonal antibody	Invitrogen	A32723
Alexa Fluor 488 goat anti-mouse secondary polyclonal antibody	Invitrogen	A32732
Anti-GAPDH	Abcam	ab199553
Anti-β-actin	Abcam	Ab170325
HRP Goat Anti-Rabbit IgG (H + L)	ZSGB-BIO	ZB-2301
Chemicals, peptides, and recombinant proteins		
MK-2206-2HCl	MCE	HY-10358
SB203580	MCE	HY-10256
U0126	MCE	HY-12031A
BAPTA-AM	MCE	HY-100545
Thapsigargin	MCE	HY-13433
KN-93 Phosphate	MCE	HY-15465B
Staurosporine	MCE	HY-15141
RIPA buffer	Yeasen	20115ES60
Protein Molecular Weight Marker	thermo	26612
Protein Molecular Weight Marker	thermo	26616
Paraformaldehyde	Sigma	P6148
PDMS curing agent	Dow corning Corp	sylgard184
Sulfo-SANPAH	Pierce	22589
Type I collagen	Gibco	A1048301
Trizol reagent	Thermo	15596026
rhodamine	Sigma	79754
FuGENE® HD Transfection Reagent	Progema	E2311
T4 DNA ligase	NEB	M0202L
Trizol reagent	Thermo	15596026
Critical commercial assays		
mMESSAGE mMACHINE SP6 transcription kit	Invitrogen	AM1304
MEGAclear Transcription Clean-Up Kit	Invitrogen	AM1908
FastQuant RT Kit (With gDNase)	Tiangen	KR106-03
Dual-Luciferase® Reporter Assay System	Promega	E1910
Super ECL Plus	Huaxingbio Science	HXP1868
Q5 High-fidelity PCR kit	NEB	NEB
T7 RNA Polymerase	Promega	P2075
SP6 RNA Polymerase	Promega	P1085

(*Continued on next page*)

Continued

REAGENT or RESOURCE	SOURCE	IDENTIFIER
Experimental models: Cell lines		
MDCK	ATCC	NBL-2
Experimental models: Organisms/strains		
Zebrafish AB	Nanjing EzeRinka Biotechnology	N/A
Hsf1a$^{ihb294/+}$ (AB)	CZRC	CZ1203
Oligonucleotides		
hsp70: FP AGCTGGAGCAGGTGTGTAAC	qRT-PCR	N/A
hsp70: RP GGGGAAGAAGTCCTAATCCACC	qRT-PCR	N/A
gapdh: FP AGTCAACGGATTTGGCCGTA	qRT-PCR	N/A
gapdh: RP CCGTTCTCAGCCTTGACTGT	qRT-PCR	N/A
Spaw:FP CCGCTGTACATGATGCAGTT	*in situ* hybridization	N/A
Spaw:RP GTAAGCGTGGTTTGTTGGGT	*in situ* hybridization	N/A
Charon: FP AAGACTTTGAATCCTCCGGG	*in situ* hybridization	N/A
Charon: RP ACGTTTCTGTTTGCAGGGAC	*in situ* hybridization	N/A
Clmc2: FP TTGTGCAGTTATCAGGGCTC	*in situ* hybridization	N/A
Clmc2: RP TTAACAGTCTGTAGGGGGCA	*in situ* hybridization	N/A
Hsf2: FP ATGAAACACAGCTCGAACG	For PCS2-HSF2	N/A
Hsf2: RP TCAGATATCAAGCGGTGGTGT	For PCS2-HSF2	N/A
Recombinant DNA		
PCS2-6myc-hsf2	This paper	N/A
pHSE-luc	Clontech	VT001502
pRL-CMV	promega	E2261
Software and algorithms		
ImageJ	NIH	N/A
Origin	OriginLab	N/A
LAS_X	Leica	N/A
Adobe Illustrator	Adobe	N/A

RESOURCE AVAILABILITY

Lead contact

Further information and requests for resources and reagents should be directed to and will be fulfilled by the lead contact, Jing Du (dujing@buaa.edu.cn).

Materials availability

Zebrafish mutants generated in this study are available from lead contact upon request.

Data and code availability

Data reported in this paper will be shared by the lead contact upon request. This paper does not report original code. Any additional information required to reanalyze the data reported in this paper is available from the lead contact upon request.

EXPERIMENTAL MODEL AND STUDY PARTICIPANT DETAILS

Cell and fish maintenance

MDCK cells and human MSCs were grown in DMEM culture medium supplemented with 10% fetal bovine serum (Gibco), 100 mg/mL streptomycin and 100 units/ml penicillin (Gibco) in a humidified incubator at 37°C and with 5% CO_2 atmosphere. All zebrafish husbandry was performed under standard conditions in accordance with institutional and national ethical and animal welfare guidelines. Collected embryos were grown at 28.5°C. Zebrafish used in this study included wild-type AB strain, mutant line Hsf1a$^{ihb294/+}$.

CRISPR/Cas9-mediated knockdown in zebrafish

CRISPR/Cas9-mediated knockdown zebrafish were obtained from the China Zebrafish Resource Center. Wild-type AB/TU and mutant zebrafish were raised and maintained under standard conditions. Zebrafish embryos were obtained by artificial insemination and reared at 28°C. All animal experiments were conducted in accordance with the Guiding Principles for the Care and Use of Laboratory Animals and were approved by the Institute of Hydrobiology, Chinese Academy of Sciences.

Zebrafish mutant line CZ1203/ihb294 is between 412 bp to 421 bp of the wild-type hsf1 coding sequence, TGGCCAGTTT, is deleted. The mutated hsf1 codes for a truncated protein containing 152 aa, 133 aa of which is identical to wildtype hsf1.

METHOD DETAILS

Antibodies and reagents

Antibodies against HSF1, anti-HSF1 (phospho S326) were purchased from Abcam. Monoclonal anti-Acetylated Tubulin antibody was purchased from Sigma. Alexa Fluor 546-labeled goat anti-rabbit secondary polyclonal antibody and Alexa Fluor 488-labeled goat anti-mouse secondary polyclonal antibody were purchased from Life Technology. Monoclonal antibody against GAPDH, horseradish peroxidase (HRP)-coupled goat anti-rabbit secondary polyclonal antibody and horseradish peroxidase (HRP)-coupled goat anti-mouse secondary polyclonal antibody were obtained from Abcam.

Inhibitors of Akt (MK-2206 2HCl), MAPK (SB203580), MEK (U0126), CaMKII (KN-93 Phosphate), PKC (Staurosporine) and Ca^{2+} (BAPTA-AM), were purchased from MCE.

Flow chamber

A rectangular parallel plate perfusion chamber, designed and presented by professor Jeng-Jiann Chiu Lab in the National Health Research Institutes of Taiwan, was used for fluid shear stress exposure. This system comprises a transparent polymethylmethacrylate plate, two silastic rubber gaskets, and a standard glass coverslip. The coverslip with near 90% confluent monolayer of MDCK cells was mounted over the groove with the cells facing the inside, and an approximate 200 μm high gap was formed over the MDCK cells. Then we collected the treated samples from each condition for the following analyses.

Mechanical stretch

PDMS curing agent (sylgard184; Dow corning Corp) was mixed with base agent in a mass ratio of 10:1 in 50 mL centrifugal tubes, and centrifuged in a bench-top centrifuge to remove air bubbles, which was subsequently cast onto a single-well Petri dish (35 × 10 mm, Corning) and cured at 65°C for 12 h. The PDMS substrates were oxidized in an oxygen plasma cleaner, which generated silanol group (Si-OH) on the surface of the PDMS, then sterilized by UV radiation for 2 h, coated with fibronectin and left in a laminar flow cabinet for at least 2 h. Then, MDCK cells achieving 90% confluence were subjected to mechanical stress with the Cyclic Stress Unit. The unit was placed in a humidified incubator with 5% CO_2 at 37°C. Cyclic deformation (20 cycles/min) and up to 10% elongation was applied. Then we collected the treated samples from each condition for the following analyses.

Hypergravity stress

MDCK Cells (5×10^4) were placed in an incubator at 37°C with 40 ×g with hypergravity treatments using a centrifuge. Samples were collected at 30 min, 1 h, 2 h and 4 h. Then, the treated samples from each condition were used for the following analyses.

Substrate stiffness

Polyacrylamide gels with variable Young's moduli were prepared by mixing acrylamide and diacrylamide in different proportions.[36] Drops of polymerizing gel solution were placed on glutaraldehyde-treated aminosilanized coverslips, which covalently bound the PA. Chlorosilanized coverslips were placed on top of the PA, and weights were added to ensure that the gel thickness was defined by the spacer bead diameter. Then, the gel was covered by sulfosuccinimidyl-6-[4′-azido-2′-nitrophenylamino] hexanoate (Sulfo-SANPAH; Pierce). After exposure to UV light for 10 min twice, the polyacrylamide sheet was washed twice and incubated with a solution of type I collagen (0.2 mg/mL; Gibco BRL) overnight at 4°C.

Immunofluorescence staining and confocal microscopy

MDCK cells were fixed with 4% paraformaldehyde (PFA), permeabilized with 0.5% Triton X-100, blocked with 5% BSA for 1 h at room temperature. Then, cells were probed with antibodies overnight, followed by incubation with Alexa Fluor 546-labeled goat anti-rabbit secondary polyclonal antibody and Alexa Fluor 488-labeled goat anti-mouse secondary polyclonal antibody for 1 h. After washing with PBST for several times, cell nuclei were stained by DAPI. Then, the fluorescent images were captured with a ×63 objective mounted on a LSM710 confocal microscope.

The zebrafish embryos were fixed in BT fixative buffer [4% paraformaldehyde, 0.15 mM $CaCl_2$, 4% sucrose in 0.1 M PBS (pH 7.3)] overnight at 4°C. After being rinsed 3–5 times with PBST, embryos were blocked at room temperature for 1 h in 5% BSA and 1% DMSO in PBST. Embryos were then incubated overnight at 4°C with antibodies. After washing with PBST three times, embryos were incubated overnight at 4°C with

Alexa Fluor 488-conjugated AffiniPure Donkey anti-mouse IgG and Alexa Fluor 546-conjugated AffiniPure Goat anti-rabbit IgG. Embryos were then washed with PBST and stained by DAPI. Then, embryos were transferred into an anti-fade reagent and stored at 4°C for up to 3 days. Immunostained embryos were imaged under a Zeiss 710META laser scanning confocal microscope with a 63×objective. A KV/cilia image was a sum of multiple focal planes (z series), combined using ImageJ. The fluorescent intensity was analyzed using Image-Pro Plus 6.0.

Quantitative real-time PCR (qRT-PCR)

The qRT-PCR was conducted as described previously.[58] Total RNA was isolated using the Trizol reagent (Invitrogen). For qRT-PCR analysis, it was performed in accordance with the manufacturer's instructions using FastQuant RT Kit (With gDNase) (Tiangen). Relative mRNA levels of each gene were analyzed according to the comparative Ct method and were normalized to the expression of GAPDH. The following sets of primers were used in the PCR amplification:

hsp70 (forward, 5'-AGCTGGAGCAGGTGTGTAAC-3'; reverse, 5'-GGGGAAGAA.

GTCCTAATCCACC-3', GTCCTAATCCACC-3'). GAPDH (forward, 5'-AGTCAACGGATTTGGCCGTA-3'; reverse, 5'-CCGTTCTCAGCCTT GACTGT-3').

For all the qRT-PCR experiments, the correlation coefficient and amplification efficiency in the reaction using each primer are 0.97–1.02 and more than 97.9%, respectively.

MO oligonucleotides injections

For totally knockdown, morpholinos (Gene Tools) were injected into the yolk of one-cell stage embryos. DFCs specific knockdown was performed as described previously.[59] Briefly, the morpholino was mixed with rhodamine (Sigma) and injected into the yolk at the 512-cell stage. Then, at 60–70% epiboly stages, the embryos with red fluorescence in DFCs were sorted and raised for further investigations.

mRNA injections

In order to synthesize hsf2 mRNA *in vitro*, we used restriction endonuclease and T4 ligase to integrate hsf2 gene into PCS-6MYC vector and synthesized hsf2 mRNA *in vitro* using mMESSAGE mMACHINE kit (Thermo, AM1340). Then the wild type zebrafish embryo was injected into the yolk at 1–4 cell stage, and the total protein was extracted at 24 h for follow-up experiment.

Double-luciferase report gene experiment

RL (500 ng/ul,clontch) and pHSE-luc(500 ng/ul,clontch) were cotransfected into MDCK cell line using FuGENE HD for 24 h. We use shear stress stimulate cell 1 h after transfection. The cells were lysed using 1X passive lysate. Firefly luciferase was used as a transfection control group, and the luciferase activity was measured using a dual luciferase reporter assay system.

Western blotting

Western blotting was conducted as described previously.[36] Proteins (40 μg) from cell homogenates were separated on a 10% SDS-polyacrylamide gel and electrotransfered to polyvinylidene fluoride membranes (Millipore). Each membrane was washed with Tris-buffered saline Tween 20, blocked with 5% skim milk power for 1 h, and incubated with appropriate primary antibodies at dilutions recommended by the supplier. Membranes were washed in TBST and probed with an appropriate HRP conjugated secondary antibody. The oxidase components were detected by chemiluminescence (Super ECL Plus, Huaxingbio Science).

Whole-mount *in situ* hybridization

Whole-mount *in situ* hybridization analyses were performed as described previously.[27] The primers used for probes synthesis are as follows: southpaw, CCGCTGTACATGATGCAGTT and GTAAGCGTGGTTTGTTGGGT; charon, AAGACTTTGAATCCTCCGGG and ACGTTTCTGT TTGCAGGGAC; cmlc2, TTGTGCAGTTATCAGGGCTC and TTAACAGTCTGTAGGGGGCA.

QUANTIFICATION AND STATISTICAL ANALYSIS

ImageJ software was used to measure fluorescence intensity and gray value. All quantitative experiments were performed with at least three independent biological repeats. Results were expressed as means ± SEM. Significance of differences between means was evaluated by Student's *t* test. ***$p < 0.001$, **$p < 0.01$, *$p < 0.05$; n.s., not significant.